Immunity, Vol. 22, 355–370, March, 2005, Copyright ©2005 by Elsevier Inc. DOI 10.1016/j.immuni.2005.02.004

Granzyme A Induces Caspase-Independent Mitochondrial Damage, a Required First Step for Apoptosis

Denis Martinvalet, Pengcheng Zhu, and Judy Lieberman*
The CBR Institute for Biomedical Research and Department of Pediatrics
Harvard Medical School
Boston, Massachusetts 02115

Summary

Granzyme A (GzmA) triggers cell death with apoptotic features by targeting the endoplasmic reticulum-associated SET complex, which contains the GzmA-activated DNase NM23-H1, its inhibitor SET, and Ape1. The SET complex was postulated to translocate to the nucleus in response to oxidative stress and participate in its repair. Because mitochondrial damage is important in apoptosis, we investigated whether GzmA damages mitochondria. GzmA induces a rapid increase in reactive oxygen species and mitochondrial transmembrane potential loss, but does not cleave bid or cause apoptogenic factor release. The mitochondrial effect is direct, does not require cytosol, and is insensitive to bcl-2 and caspase inhibition. SET complex nuclear translocation, which occurs within minutes of peroxide or GzmA treatment, is dependent on superoxide generation since superoxide scavengers block it. Superoxide scavengers also block apoptosis by CTLs expressing GzmA and/or GzmB. Therefore, mitochondrial damage is an essential first step in killer cell granule-mediated pathways of apoptosis.

Introduction

Granzyme A (GzmA), an abundant serine protease in cytotoxic T lymphocyte (CTL) and NK cell granules, induces a cell death pathway that is caspase independent, but has many features of apoptosis (Beresford et al., 1999; Lieberman and Fan, 2003). Targeted cells display all the morphological features of apoptosis, but bcl-2 overexpression or caspase inhibition do not block the pathway, and DNA damage occurs via single-stranded nicks, instead of by oligonucleosomal double-stranded breaks (Beresford et al., 1999; Fan et al., 2003a). Most of the intracellular GzmA targets identified so far (SET [Beresford et al., 1997], HMG-2 [Fan et al., 2002], Ape1 [Fan et al., 2003b], core and linker histones [Zhang et al., 2001b], lamins [Zhang et al., 2001a]) are not targeted during caspase-dependent apoptosis.

A special target of GzmA is a 270–420 kDa endoplasmic reticulum (ER)-associated complex, termed the SET complex, which contains the GzmA-activated DNase NM23-H1, the protein phosphatase PP2A inhibitor pp32, and three GzmA substrates—the nucleosome assembly protein SET, the base excision repair enzyme Ape1, and the DNA bending protein HMG-2 (Beresford et al., 2001). The SET complex translocates to the nucleus of target cells within minutes of GzmA loading or CTL attack (Fan et al., 2003a). Although the normal function of the SET complex is not known, its constituent proteins have been highly implicated in tumorigenesis. They have been linked to diverse functions, including chromatin modification, transcriptional activation of protooncogenes, DNA repair, and mRNA stability (Brennan et al., 2000; Demple et al., 1991; Ma et al., 2002; Seo et al., 2001; Shikama et al., 2000). We postulated, based on the properties of its known components, that the SET complex participates in the oxidative stress response by moving to the nucleus, where it activates expression of key early response genes and repairs oxidative DNA damage (Fan et al., 2003b).

Mitochondrial damage is a key initial step in caspase-dependent apoptosis, including that induced by GzmB, in which it is triggered by proteolytic cleavage of bid (Alimonti et al., 2001; Barry et al., 2000; Gross et al., 1999; Heibein et al., 2000; Li et al., 1998; Luo et al., 1998; Marchetti et al., 1996; Sutton et al., 2000). During caspase-induced apoptosis, mitochondrial function is completely disrupted, as evidenced by a loss of the mitochondrial transmembrane potential ($\Delta\psi$) and an increase in reactive oxygen species (ROS). Moreover, the outer mitochondrial membrane is disrupted, leading to the release of apoptogenic factors, including cytochrome c (Kluck et al., 1997; Krippner et al., 1996; Yang et al., 1997), HtrA2/Omi (Hegde et al., 2002; Martins et al., 2002; van Loo et al., 2002; Verhagen et al., 2002), endonuclease G (endoG) (Parrish et al., 2001; van Loo et al., 2001), Smac/Diablo (Du et al., 2000; Verhagen et al., 2000), and apoptosis inducing factor (AIF) (Susin et al., 1999), from the intermembrane space. Some features of mitochondrial damage can also be induced independently of the caspases by both GzmB and GzmC (Heibein et al., 1999; Johnson et al., 2003; MacDonald et al., 1999; Thomas et al., 2001).

In this study, we looked at the mitochondrial effects of GzmA. We find that although GzmA does not cleave bid or disrupt the mitochondrial outer membrane (MOM) to cause release of the caspase pathway apoptogenic factors, it directly causes a rapid increase in ROS and loss of $\Delta\psi$ in a caspase-independent manner that is not blocked by bcl-2 overexpression or by caspase inhibitors. Moreover, mitochondrial damage is key to SET complex nuclear translocation and GzmA induction of apoptosis. Peroxide treatment causes some of the SET complex to move rapidly into the nucleus. When cells are treated with superoxide scavengers, the SET complex does not translocate, and target cells are protected from GzmA-mediated cell death. Moreover, the same superoxide scavengers also block cell death induced by CTLs expressing GzmB.

Results

GzmA Directly Induces a Rapid and Sustained Increase in Intracellular ROS and Loss of $\Delta\psi$

During target cell attack by CTLs and NK cells, granzymes are delivered into the target cell cytosol by

*Correspondence: lieberman@cbr.med.harvard.edu

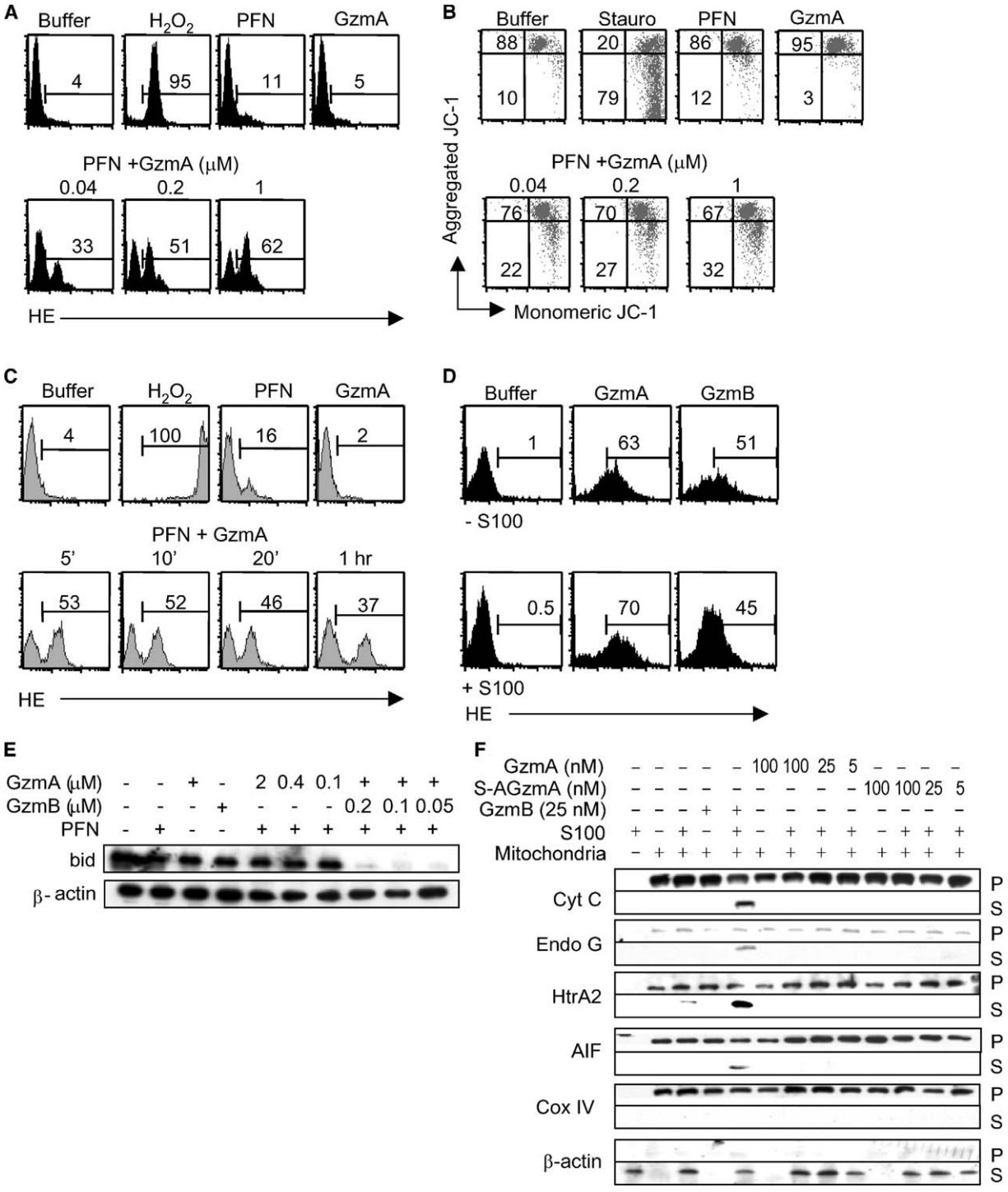

Figure 1. GzmA Induces a Rapid Increase in Intracellular ROS and Mitochondrial Transmembrane Potential Loss without MOM Rupture

(A) GzmA loading of K562 cells with PFN induces a dose-dependent increase of ROS. Cells, preloaded with HE, were analyzed by flow cytometry 1 hr after incubation in buffer alone or buffer with H_2O_2 (positive control), a sublytic concentration of PFN, GzmA alone, or PFN plus GzmA at indicated concentrations. The numbers indicate the percentage of fluorescent cells.

(B) GzmA treatment of K562 cells induces a dose-dependent loss of $\Delta\psi$. Cells stained with the potentiometric dye JC-1 were treated overnight with 0.1 μM staurosporine (stauro, positive control), or for 1 hr with PFN and/or GzmA as in (A). The numbers indicate the percentage of cells in the upper-right quadrant with intact $\Delta\psi$ and those in the lower-right quadrant with loss of $\Delta\psi$.

(C) The increase in ROS after GzmA loading of K562 cells with PFN occurs rapidly. Cells were treated for the times indicated and stained for ROS.

(D) GzmA triggers an increase in ROS directly on isolated mitochondria. Mouse liver mitochondria were treated with GzmA or GzmB in the presence or absence of cytosolic S100 fraction. Addition of cytosol did not affect ROS generation by GzmA or GzmB.

perforin (PFN). To assess the effects of GzmA on mitochondrial function, K562 cells were treated with recombinant GzmA plus native purified PFN and were analyzed by flow cytometry for changes in ROS and $\Delta\psi$. GzmA loading by PFN induced a dose-dependent accumulation of intracellular ROS, as measured by detection of the conversion of hydroethidine (HE) to fluorescent ethidium (Figure 1A). Treated cells also exhibited a dose-dependent decrease in $\Delta\psi$, assayed by the change in fluorescence of the membrane potential-sensitive dye 5,5′,6,6′-tetrachloro-1,1′,3,3′-tetraethylbenzimidazolylcarbocyanine (JC-1) (Figure 1B). Similar results were found by staining with the dye 3,3′ dihexyloxacarbocyanine iodide ($DiOC_6$) (data not shown). ROS accumulation and loss of $\Delta\psi$ required GzmA delivery by PFN, as treating cells with either GzmA or PFN alone had little effect. Both changes required enzymatically active GzmA, since PFN-mediated delivery of the inactive enzyme produced by mutating the active site Ser184 to Ala (S-AGzmA) did not alter ROS or $\Delta\psi$ (data not shown). GzmA increases intracellular ROS very rapidly (within 5 min), and the increase is maintained for at least 2 hr (Figure 1C and data not shown). The total pool of accumulated ROS increases over time, as seen by the increase in mean fluorescence intensity (MFI) of the ROS indicator dye between 20 min (MFI, 12), 1 hr (MFI, 30), and 2 hr (MFI, 52). Similar results and kinetics were obtained by using Jurkat cells (data not shown).

GzmB induces mitochondrial damage by two distinct pathways. One pathway, whose molecular basis is unknown, involves direct action on mitochondria to induce increased ROS and loss of $\Delta\psi$, but not release of cytochrome c and other intermembrane proapoptotic factors (Heibein et al., 1999; MacDonald et al., 1999; Thomas et al., 2001). The other requires cleavage and activation of cytosolic bid at a site distinct from caspase-8, leading to release of proapototic factors in addition to increased ROS and loss of $\Delta\psi$ (Alimonti et al., 2001; Barry et al., 2000; Gross et al., 1999; Heibein et al., 2000; Li et al., 1998; Luo et al., 1998; Marchetti et al., 1996; Sutton et al., 2000). These two pathways can be distinguished by treating isolated mitochondria with GzmB in the presence or absence of cytosolic S100 fraction as a source of bid. We confirmed these results for GzmB (Figures 1D and 1E and data not shown). Despite the well-documented role of bid in activating apoptotic mitochondrial damage, we confirmed the previous finding (Alimonti et al., 2001) that the extent of ROS generation and $\Delta\psi$ loss was not augmented by adding cytosol as a source of bid. This suggests that both bid-dependent and -independent GzmB mitochondrial pathways independently disrupt mitochondrial electron transport. We also looked at the effect of GzmA on freshly purified mouse liver mitochondria in the presence and absence of cytosol. GzmA directly induced increased ROS and loss of $\Delta\psi$ (Figure 1D, data not shown). Adding S100 cytoplasmic fraction did not reproducibly increase the rate or magnitude of ROS induction or alter the loss of $\Delta\psi$. Therefore, GzmA directly causes mitochondrial disruption without requiring cytosolic factors. Moreover, the mitochondrial effect of recombinant human GzmA is not cell type or species specific since it occurs in human K562 and Jurkat cells as well as in mouse liver mitochondria. Similar results were obtained when ROS production and loss of $\Delta\psi$ were monitored with 2′,7′-diclorofluorescein diacetate (DCFDA) and $DiOC_6$, respectively (data not shown).

GzmA Does Not Cleave Bid or Trigger Release of Mitochondrial Proapoptotic Molecules

Truncated bid, produced by caspase or GzmB cleavage, causes mitochondrial proapoptotic factor release. However, GzmA does not cleave bid in cytosolic extracts (data not shown), and loading cells with GzmA and PFN does not lead to bid cleavage, while loading with GzmB and PFN does (Figure 1E). Moreover, GzmA does not appear to disrupt the ability of the MOM to contain intermembrane proteins. Treatment of purified mitochondria with GzmA in the presence or absence of S100 cytoplasmic fraction does not trigger the release of apoptogenic factors from the mitochondrial intermembrane space (Figure 1F). As expected, the catalytically inactive S-AGzmA also does not cause mitochondrial proteins to be released. This is in contrast to GzmB treatment, in which all four of the five known intermembrane apoptogenic factors studied (cytochrome c, HtrA2/Omi, endoG, and AIF) were detected in the supernatant following treatment, provided that S100 fraction, a source of bid, was added. The release of Smac/DIABLO by GzmB plus S100 was difficult to verify because of the poor specificity of the antibody. These data show that GzmA initiates a pathway of mitochondrial disruption that is distinct from that caused by caspase activation. Generation of ROS and loss of $\Delta\psi$ occur in response to GzmA in the absence of added cytosolic factors and without apparent dissolution of the MOM.

Granzyme A Induces ROS Accumulation in Target Cells upon CTL Attack

To test whether GzmA release by cytotoxic T cells results in ROS production in target cells, we used HE staining and confocal fluorescence microscopy to detect ROS in primary T cell:target cell conjugates. P14 mice expressing a transgenic T cell receptor that recognizes the LCMV antigen gp33 in the context of class I major histocompatibility complex (Pircher et al., 1989) were bred with GzmB cluster knockout mice, which express only GzmA at high levels (Heusel et al., 1994; Pham

(E) GzmA does not cleave bid when delivered by PFN into K562 cells. GzmB serves as a positive control for bid cleavage.
(F) GzmA, unlike GzmB, does not induce MOM rupture, as monitored by apoptogenic factor release. Isolated mitochondria were treated for 30 min with GzmA, catalytically inactive S-AGzmA, or GzmB in the presence or absence of cytosol (S100). Immunoblots of the mitochondrial pellet (P) and reaction supernatants (S) were probed with antibodies to cytochrome c (Cyt c), the serine protease HtrA2, endonuclease G (Endo G), and apoptosis inhibitory factor (AIF). Cytosolic β-actin and the mitochondrial internal protein cytochrome c oxidase IV (Cox IV) serve as fractionation controls. These data are representative of three independent experiments.

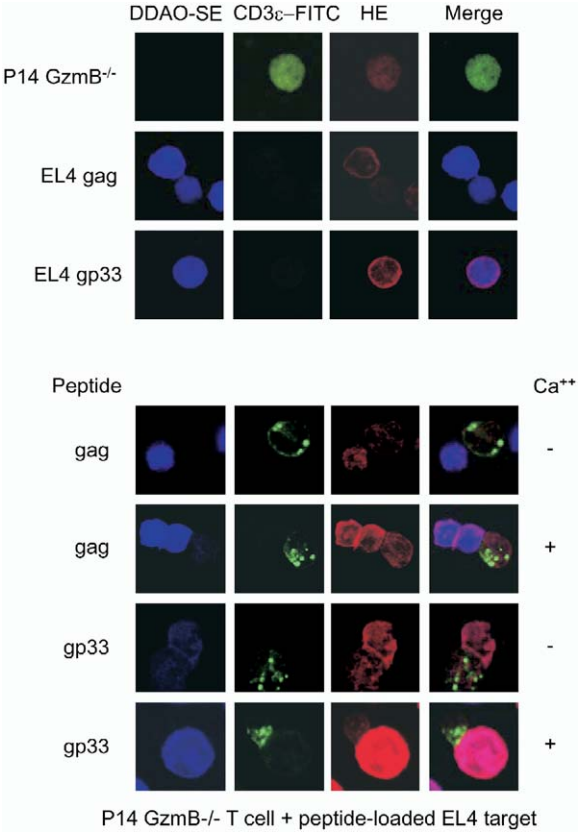

Figure 2. CTL Attack Induces ROS Production in EL4 Target Cells

EL4 target cells, pulsed with irrelevant control peptide (gag) or with the specific LCMV gp33 peptide, were stained with the cell marker dye CellTrace Far Red DDAO-SE. GzmB$^{-/-}$ P14 CTL cells were stained with FITC-conjugated anti-CD3ε. All cells were further stained for ROS with HE just before analysis by confocal microscopy. The top panels show cells from slides with either target cells or CTLs alone. In the bottom panels, the target and effector cells were separately stained and then allowed to form conjugates for 30 min in Ca^{2+}-free buffer before incubation in Ca^{2+}-free (plus EGTA) or Ca^{2+}-containing buffer for 1 min, staining with HE, and confocal microscopy analysis. CTLs trigger ROS production in target cells bearing gp33 specific peptide, but not the nonspecific gag peptide, only in the presence of extracellular Ca^{2+}, which is required for granule release. These data are representative images from one of four independent experiments.

et al., 1996) . CD8^{+} CTLs derived from P14xGzmB$^{-/-}$ mice were used as effector cells against EL4 target cells pre-pulsed with either specific gp33 peptide or a control irrelevant HIV gag peptide. Before the cells were mixed, CTLs were stained with antibody to CD3ε, and EL4 cells were labeled with CellTrace Far Red dye (DDAO-SE) (Figure 2). The effector and target cells were incubated together for 30 min in calcium-free medium to allow conjugates to form, and cell death by granule exocytosis was then triggered synchronously by adding Ca^{2+}. Within 1 min of adding Ca^{2+}, there was a dramatic increase in ROS production in gp33 peptide-loaded EL4 cells that was not seen in control peptide-loaded cells. ROS staining 5 min after initiating granule exocytosis was indistinguishable from that seen after 1 min (data not shown). If granule exocytosis was prevented by chelating Ca^{2+} with EGTA, there was no increase in ROS production, even in the presence of specific peptide. As the GzmB cluster knockout mice efficiently express only GzmA, these data strongly suggest that PFN-mediated delivery of GzmA by CTL granule exocytosis induces rapid ROS production in the target cell. Moreover, both murine and human GzmA trigger rapid ROS production in target cells.

GzmA-Induced ROS Accumulation and $\Delta\psi$ Loss Are Insensitive to bcl-2 Overexpression and Occur Independently of Caspase Activation

GzmA-activated cell death is caspase independent, and our results in Figure 1 suggest that mitochondrial damage also occurs by a different pathway than that induced by caspase activation. Overexpression of bcl-2 inhibits caspase-dependent mitochondrial damage. To test the role of the bcl-2/caspase pathway in GzmA-induced mitochondrial disruption, we examined ROS production and mitochondrial $\Delta\psi$ in Jurkat cells transfected to overexpress bcl-2 (Figure 3A). GzmA loading caused a dose-dependent increase in intracellular ROS in bcl-2-overexpressing Jurkat cells that was indistinguishable from the increase seen in control cells transfected with the empty vector (Figure 3B). As expected, ROS production in Jurkat and Jurkat-bcl-2 cells required treatment with both GzmA and PFN. In addition, the disruption of $\Delta\psi$ seen after the addition of GzmA plus PFN was also insensitive to bcl-2 overexpression (Figure 3C). Together, these results demonstrate that delivery of GzmA by PFN into Jurkat cells disrupts mitochondrial function via a pathway that cannot be blocked by bcl-2 overexpression. Unlike for GzmA-induced mitochondrial damage, bcl-2 overexpression dampens GzmB- or staurosporine-induced mitochondrial damage (Figures 3B and 3C), confirming that overexpressing bcl-2 inhibits caspase-dependent mitochondrial damage.

To probe further whether the observed ROS accumulation and loss of $\Delta\psi$ in Jurkat cells treated with GzmA is caspase dependent, we treated cells with the pan-caspase inhibitor zVAD-fmk and the caspase-3 inhibitor DEVD-fmk before exposing the cells to GzmA and PFN. Caspase inhibition did not decrease the accumulation of ROS (Figure 3D) or the loss of $\Delta\psi$ (Figure 3E) in response to GzmA and PFN. The caspase inhibitors partially blocked the loss of $\Delta\psi$ induced by UV treatment, demonstrating that caspase-dependent pathways of mitochondrial damage were in fact inhibited at the indicated doses of zVAD-fmk and DEVD-fmk. These data confirm that mitochondrial damage induced by GzmA is caspase independent.

GzmA-Induced ROS Accumulation and Loss of $\Delta\psi$ Are Attenuated by Inhibiting the Permeability Transition Pore and by Antioxidants and Free Radical Scavengers

We next assessed whether the mitochondrial effects of GzmA involve opening the mitochondrial permeability transition (PT) pore. When the mitochondrial PT pore opens, the mitochondrial inner membrane potential collapses as a consequence of dissipating the proton gradient generated in the mitochondrial intermembrane

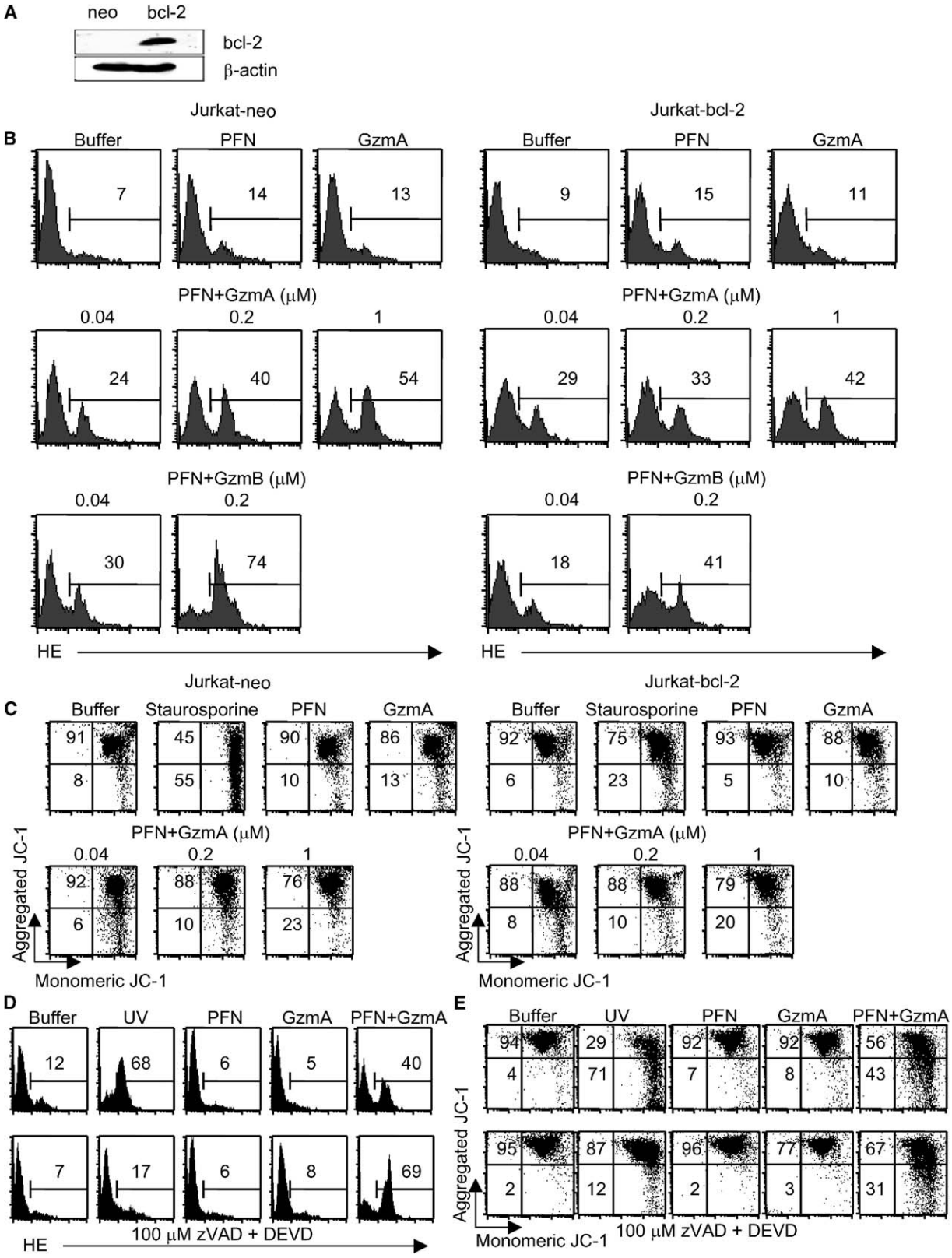

Figure 3. GzmA-Induced ROS and Loss of $\Delta\psi$ Is bcl-2 Insensitive and Caspase Independent

(A) bcl-2 expression is greatly increased in Jurkat cells stably transfected to express *bcl-2*. Whole-cell lysates from Jurkat-neo cells transfected with the empty vector and Jurkat-bcl-2 cells were analyzed by immunoblot for bcl-2 and β-actin expression.

(B) GzmA-induced increase in ROS measured by HE staining is not attenuated in Jurkat-bcl-2 cells. Cells were treated as indicated for 1 hr at 37°C before HE staining. bcl-2 overexpression inhibits ROS generation by GzmB.

(C) GzmA-induced loss of $\Delta\psi$, detected by JC-1 staining, is not affected by bcl-2 overexpression.

(D and E) ROS generation and loss of $\Delta\psi$ in K562 cells after treatment with GzmA and PFN is not altered by 100 μM zVAD-fmk and 100 μM DEVD-fmk (bottom row). As expected, these caspase inhibitors interfered with UV-induced mitochondrial damage. These data are representative of three independent experiments.

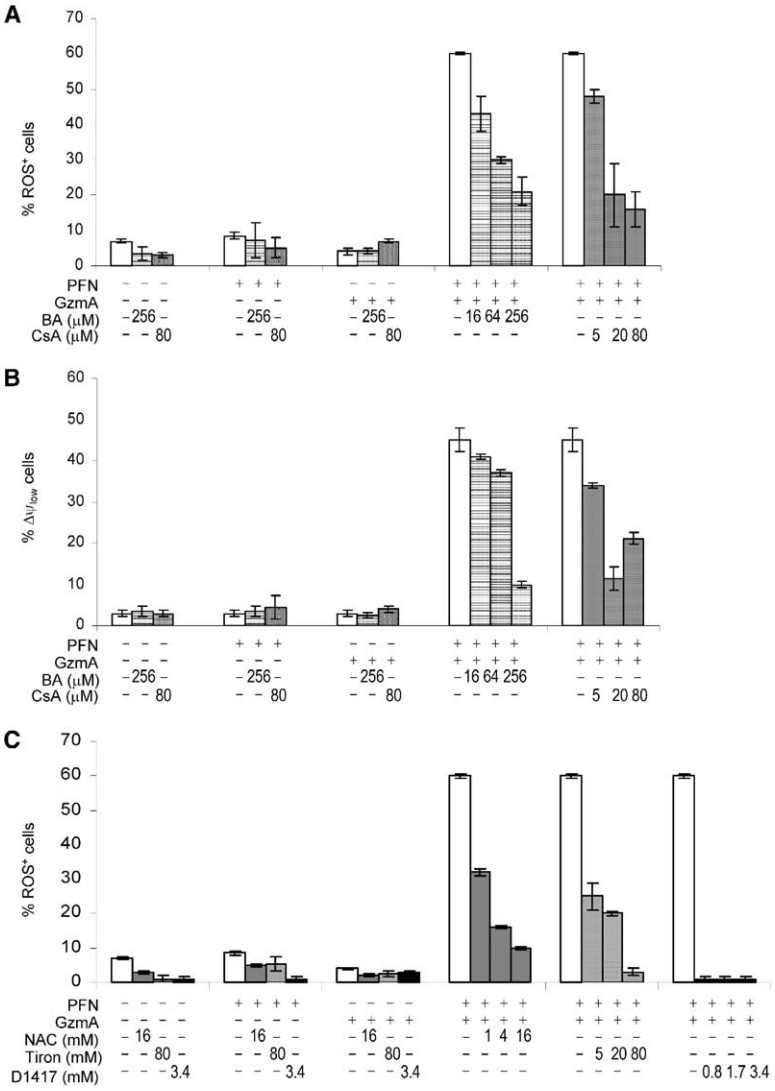

Figure 4. Mitochondrial Damage by GzmA Depends on PT Pore Opening and Can Be Inhibited by Antioxidants

(A and B) The PT pore inhibitors cyclosporine A (CsA) and bongkrekic acid (BA) inhibit (A) ROS production and (B) loss of $\Delta\psi$ after GzmA and PFN treatment of K562 cells. (C) Preincubation of K562 cells with the antioxidants N-acetyl cysteine (NAC), Tiron, and D1417 inhibits GzmA-induced increase in ROS. Similar results were obtained with Jurkat cells.

Data are means and SDs from three independent experiments.

space. Opening the PT pore uncouples the respiratory chain and leads to overproduction of superoxide anions (Kroemer et al., 1998; Zamzami et al., 1996). To determine the contribution of PT pore function on GzmA-induced ROS accumulation and loss of $\Delta\psi$, cells were loaded with GzmA in the presence of two inhibitors of the PT pore, cyclosporine A (CsA) and bongkrekic acid (BA), and ROS production and $\Delta\psi$ were measured. Both CsA and BA reduced the accumulation of ROS (Figure 4A). In addition, loss of mitochondrial $\Delta\psi$ induced by GzmA could be significantly reduced upon treatment of target cells with CsA or BA (Figure 4B). These results indicate that PT pore opening helps to stimulate production of ROS and loss of $\Delta\psi$ by GzmA.

We next investigated whether drugs that react with oxidative intermediates can reduce GzmA-induced ROS. K562 cells were incubated with dilutions of the superoxide scavengers sodium 4,5 dihydroxybenzene-1,3-disulfonate (Tiron) or sodium 3,5-dibromo-4-nitrosobenzene sulfonate (D1417) or with the antioxidant and glutathione precursor N-acetyl cysteine (NAC) beginning at maximal nontoxic concentrations, determined for each drug and cell independently as the highest concentration that does not lead to increased spontaneous cell death. The accumulation of intracellular ROS after GzmA treatment of cells could be completely reversed by incubating cells with either of the superoxide scavengers Tiron or D1417 (Figure 4C). D1417 was more effective than Tiron and required 100-fold lower concentrations for complete inhibition. NAC pretreatment also inhibited ROS accumulation, but not completely. Similar results were obtained with Jurkat cells (data not shown).

The Superoxide Scavenger Tiron Inhibits ROS Accumulation Induced by GzmA in Target Cells during CTL Attack

To test the ability of superoxide scavengers to inhibit GzmA-induced ROS production during CTL attack, EL4 target cells pulsed with specific or control peptide were preincubated in the presence or absence of Tiron before adding CD8+ CTLs from P14xGzmB$^{-/-}$ mice as de-

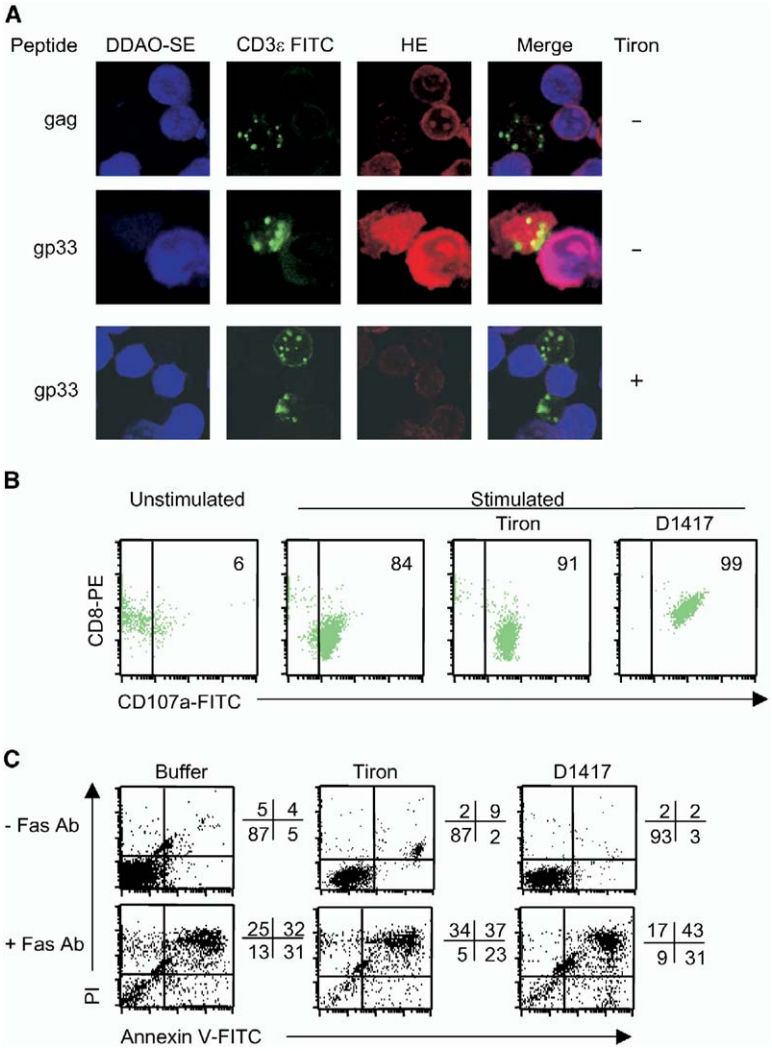

Figure 5. Tiron Inhibits ROS Accumulation in EL4 Target Cells during CTL Attack

(A) CTL granule release was triggered, in the absence or presence of the superoxide scavenger Tiron, by gp33-pulsed EL4 target cells by adding Ca^{2+} to CTL:target cell conjugates, prepared as in Figure 2. ROS production, detected by HE staining, only in response to the specific peptide, is not detected in Tiron-treated cells.

(B) CTL degranulation as measured by externalization of the lysosomal membrane protein CD107a is not inhibited by treatment with Tiron or D1417. CTLs were incubated with EL4 cells pulsed with the irrelevant gag peptide (unstimulated) or the specific gp33 peptide antigen (stimulated) for 6 hr at 37°C in the presence of CD107a-FITC. (D1417 appears to also inhibit the down-modulation of CD8 observed following T cell activation.)

(C) ROS scavengers do not block Fas-mediated cell death. Jurkat cells were pretreated with ROS scavengers or medium and then exposed to Fas antibody CH11 for 6 hr before analysis of annexin V and PI staining. These data are representative of at least four independent experiments.

scribed earlier. As previously demonstrated, the target cells show a rapid dramatic increase in the fluorescence of the ROS reporter dye HE (Figure 5A, also see Figure 2). Of note, ROS also increased in the activated CTLs exposed to gp33-armed target cells. Although all conjugates showed increased HE staining in the target cell, only some conjugates had HE-staining CTLs (i.e., see Figure 2). In these cultures, CTLs asynchronously encounter targets and may be differentially stimulated by different amounts of specific peptide-MHC complexes on the cell surface. The differential induction of ROS in CTLs may reflect a transitory or stimulus-dependent ROS increase in the CTL. In any event, when EL4 targets were preincubated with Tiron, they displayed little if any increase in HE fluorescence, even when the CTL had formed a functional immunological synapse with the target cell (Figure 5A). Neither Tiron nor D1417 treatment affected the ability of CTLs to deliver GzmA to target cells, since CTLs conjugated with peptide-pulsed EL4 cells in the presence or absence of Tiron or D1417 displayed similar levels of granule exocytosis, as measured by an in vitro degranulation assay (Figure 5B). This assay is based on the externalization of the cytotoxic granule integral membrane protein CD107a (LAMP-1, also expressed on lysosomes), when the granule membrane fuses with the plasma membrane during granule exocytosis (Betts et al., 2003). These data establish Tiron and D1417 as effective inhibitors of GzmA-induced ROS accumulation in cells undergoing CTL attack.

In addition to granule-mediated apoptosis via the action of Gzms and PFN, CTLs can also induce a Gzm-independent, slower form of apoptosis by engaging death receptors, such as Fas, in certain settings, such as during the resolution of the immune response. To determine whether treatment of target cells with superoxide scavengers also inhibits the Fas pathway, Fas-expressing Jurkat cells, pretreated with buffer, Tiron, or D1417 at the maximally tolerated concentration, were examined by annexin V-PI staining 6 hr after exposure to the agonistic Fas antibody CH11 (Figure 5C). The superoxide scavengers did not inhibit Fas-mediated cell death. Therefore, although treatment of target cells with superoxide scavengers inhibits GzmA-mediated death, inhibition is specific since they do not block all killer cell pathways of apoptosis.

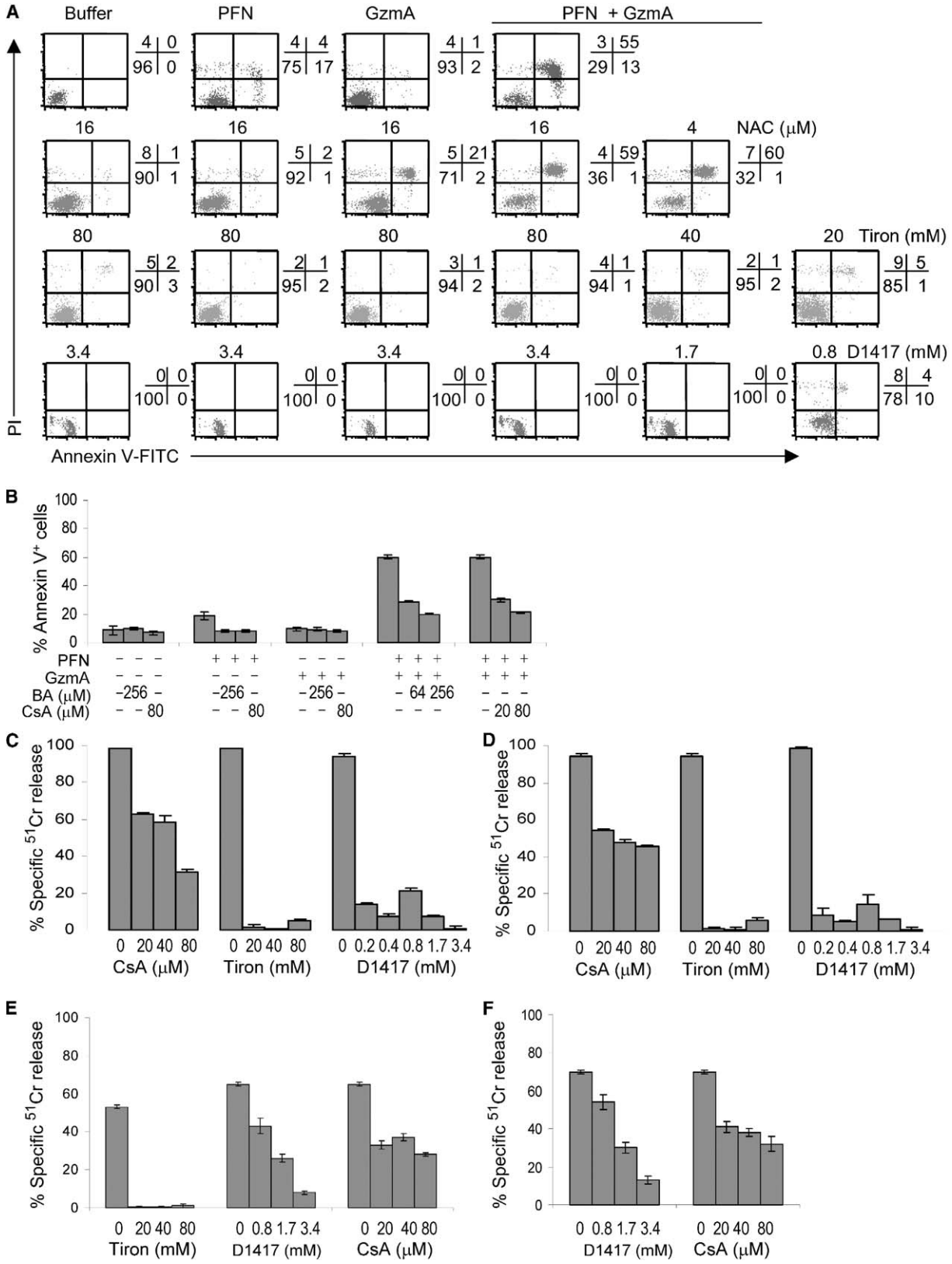

Figure 6. Inhibiting ROS Accumulation Protects Cells from GzmA- and CTL-Induced Cell Death

(A and B) K562 cells treated with (A) antioxidants or (B) PT pore inhibitors were analyzed by annexin V-PI staining for susceptibility to cell death induced by GzmA and PFN. Superoxide scavengers Tiron and D1417 completely inhibited GzmA-induced cell death, while PT pore inhibitors provided partial protection; NAC was not protective at the highest tolerated concentration.

Superoxide Scavengers Inhibit GzmA-Induced Cell Death

To determine whether increased ROS production was a byproduct of GzmA-induced cell death, or if ROS production itself was necessary for GzmA to cause cell death, we investigated the ability of GzmA to kill K562 cells in the presence of superoxide ion scavengers or PT pore inhibitors. Cells were preincubated with dilutions of each drug, starting with the highest concentration that was not toxic for the cells (data not shown), and cell death was measured 1 hr after adding GzmA and/or PFN by flow cytometry staining for annexin and PI. NAC had no protective effect on GzmA-induced cell death. However, when K562 cells were treated with the superoxide scavengers Tiron or D1417, GzmA-induced cell death was completely inhibited (Figure 6A). Since NAC primarily inhibits the accumulation of free radicals, a process downstream of superoxide production (Kroemer et al., 1998; Zamzami et al., 1996), these data suggest that superoxide generation is required for inducing cell death in response to GzmA.

GzmA loading in the presence of the PT pore inhibitors CsA or BA partially inhibited cell death (Figure 6B). At the doses used for this experiment, CsA and BA significantly inhibited both ROS production and $\Delta\psi$ loss, but the inhibition was incomplete (Figures 4A and 4B). Therefore, inhibition of GzmA-triggered cell death by different types of inhibitors correlates with the ability of the inhibitor to block ROS generation and loss of $\Delta\psi$. There are two possible explanations of the partial inhibition of cell death by PT pore inhibitors. One possibility is that GzmA-induced mitochondrial damage and cell death proceeds by both PT pore-dependent and PT pore-independent mechanisms. The other possibility is that mitochondrial damage requires PT pore opening, but the inhibitors at the highest tolerated doses only incompletely block PT pore opening. Similar results were obtained with Jurkat cells (data not shown).

The results obtained with annexin V-PI staining of GzmA- and PFN-treated target cells, were tested in the more physiological setting of CTL lysis. Cell death induced by P14xGzmB$^{-/-}$ splenic T cells against antigenic peptide-pulsed EL4 cells was assessed by ^{51}Cr release assay. As they did for GzmA and PFN treatment, Tiron and D1417 completely inhibited CTL killing (Figure 6C). At the same concentration, cells treated with Tiron or D1417 remained susceptible to Fas-mediated killing (Figure 5C), demonstrating that all forms of apoptosis may not require ROS generation. As we found for GzmA and PFN loading, CsA also partially inhibited CTL killing (Figure 6C).

Because of the effectiveness of these inhibitors at blocking GzmA-induced death, and the possible therapeutic implications of our finding, we next tested whether superoxide scavengers or inhibitors of the PT pore might also block cell death induced by the other Gzms. The CTL experiments were therefore also performed with mouse and human CTLs that express all of the Gzms. Cytotoxicity by mouse CTLs from TCR transgenic P14 mice tested against cognate peptide-coated EL4 target cells was also completely inhibited by the superoxide scavengers Tiron and D1417 and partially inhibited by CsA (Figure 6D). Human CTL lines were either lymphokine-activated killer (LAK) cells tested against concanavalin A (conA)-coated K562 targets (Figure 6E) or A2-restricted CMV peptide-specific CTLs tested against peptide-coated autologous B-LCL targets (Figure 6F). The inhibitory effects of CsA, Tiron, and D1417 on killing by human CTLs were similar to that obtained with mice cells, with complete inhibition by superoxide scavengers and partial inhibition by CsA. However, D1417 was a somewhat less effective inhibitor in human cells than it was in mouse cells, and it required about a log higher concentration for complete inhibition. Because superoxide scavengers protected against cell death induced by CTLs from both P14xGzmB$^{-/-}$ mice and GzmB+ P14 mice as well as from death by CTLs stimulated in different ways from blood lymphocytes from various healthy human donors, we can conclude that superoxide anion generation is essential for the execution of cell death by GzmB, as well as GzmA. Because the less abundant Gzms (such as GzmC and GzmM) may not have been highly expressed by these CTLs, we cannot be certain whether superoxide scavengers will also block the action of these less well-studied Gzms.

GzmA-Induced ROS Accumulation Triggers the Translocation of the SET Complex from the Cytoplasm to the Nucleus

The GzmA-activated DNase (GAAD/NM23-H1) is part of an ER-associated complex that contains pp32, SET, HMG2, and Ape1 (Fan et al., 2003a). SET inhibits the DNase. After GzmA loading with PFN or CTL attack, SET and NM23-H1 translocate into the nucleus by an unknown mechanism, and nuclear SET is degraded by GzmA cleavage, activating NM23-H1 to nick chromosomal DNA.

Since we hypothesized that the SET complex is involved in the oxidative stress response, we reasoned that ROS accumulation in response to GzmA mitochondrial damage could trigger the nuclear translocation of the SET complex. To test this hypothesis, we first asked whether H_2O_2 treatment could alter the subcellular localization of the SET complex components SET, pp32, and NM23-H1 in K562 cells. Cells were treated with H_2O_2 and separated into cytosolic and nuclear fractions, and the SET complex proteins in each fraction were analyzed by immunoblotting. SET, pp32, and NM23-H1 were detected mostly in the cyto-

(C) Complete inhibition from GzmA-induced cell death by Tiron and D1417 and partial inhibition by CsA was also demonstrated during CTL attack by using CTLs from P14xGzmB$^{-/-}$ mice to kill gp33-armed EL4 target cells. Cell killing was assessed by 6 hr ^{51}Cr release assay.
(D) The experiment in (C) was repeated by using CTLs from P14 mice in place of CTLs from P14xGzmB$^{-/-}$ mice. CTLs that expressed both GzmB and GzmA were similarly inhibited.
(E and F) The same inhibitors blocked cytolysis when tested by using human CTL effector cells against human targets. In (E), CTLs are human LAK cells against conA-coated K562 cells; in (F), CTLs are A2-restricted CMV-specific CTLs against autologous CMV-peptide-coated B-LCL. Shown are mean and SD of at least three independent experiments.

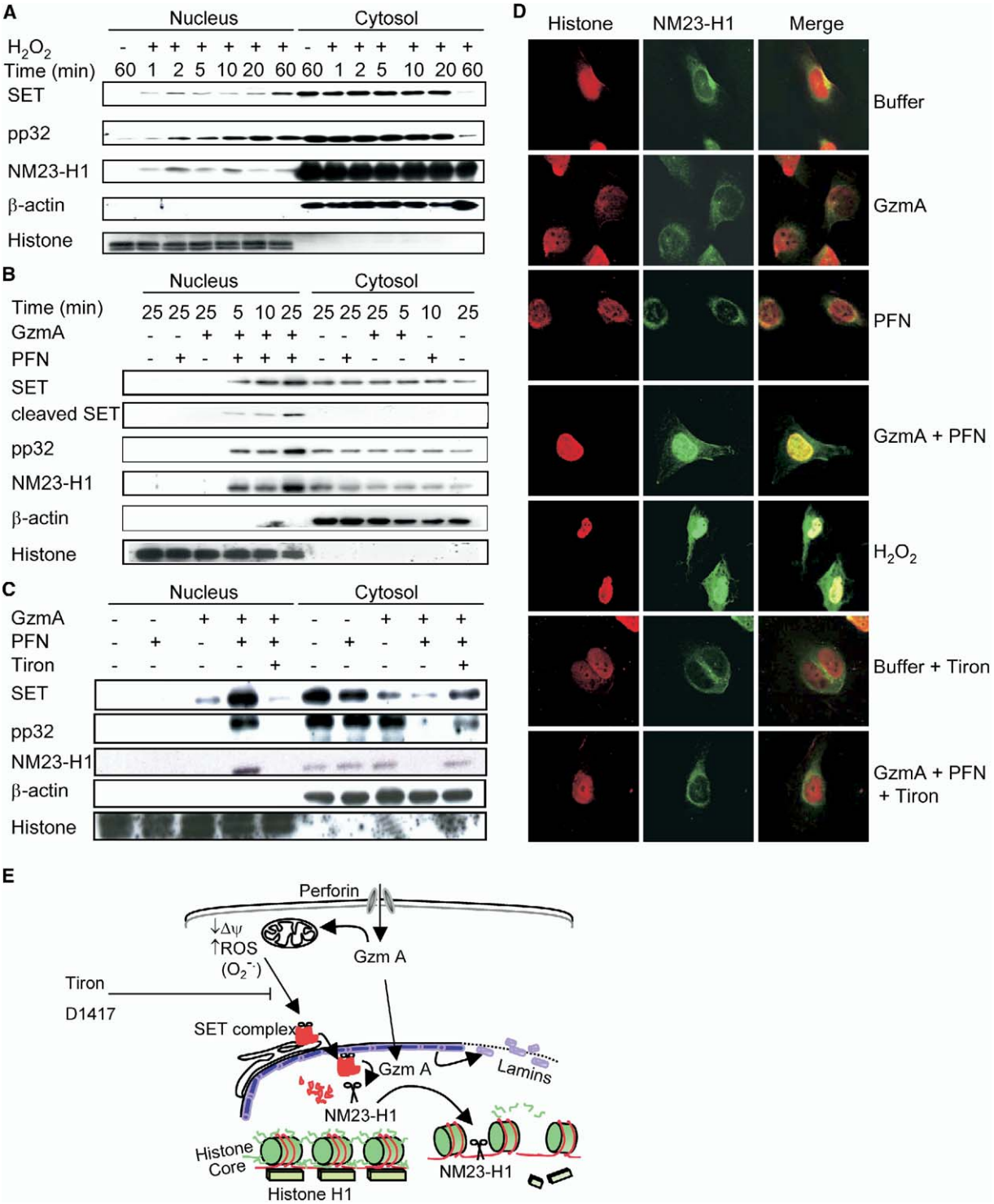

Figure 7. Oxidative Stress Triggers Nuclear Translocation of SET Complex Proteins

(A) Oxidative stress induced by adding H_2O_2 to K562 cells triggers rapid translocation of SET, pp32, and NM23-H1 from the cytoplasm to the nucleus within 1–2 min. Cell were lysed and fractionated at the indicated times after adding H_2O_2.

(B) GzmA and PFN treatment of K562 cells induces translocation of SET complex proteins. A progressive decrease in cytosolic and corresponding increase in nuclear SET complex proteins occurs over time.

(C) Tiron inhibits GzmA-induced SET complex protein translocation. Cells were treated with GzmA and PFN in the absence or presence of 80 mM Tiron. Similar results were obtained with Jurkat cells.

(D) Laser scanning confocal fluorescence microscopy confirms the nuclear translocation of the SET complex protein NM23-H1 and its inhibition by Tiron. HeLa cells, treated for 5–10 min in the absence or the presence of Tiron, were stained for NM23-H1 and histone H1 without fixation to avoid artifacts due to oxidation during fixation. These data are representative of five independent experiments.

sol in untreated K562 cells, whereas, in H_2O_2-treated cells, there was a rapid appearance of these proteins in the nuclear fraction (Figure 7A). Although most of eachof these proteins remained in the cytosolic fraction, within 1 min of H_2O_2 treatment, an increase in nuclear SET, pp32, and NM23-H1 was observed, and by 2 min, the amount in the nucleus had stabilized. The translocation appeared to be coordinate, suggesting that the whole complex translocated together. There was no trace of the control protein β-actin in the nuclear fraction, or of histone H1 in the cytoplasmic fraction, indicating complete separation of the nuclear and cytoplasmic fractions. These data strongly suggest that oxidative stress triggers the nuclear translocation of the SET complex proteins.

In agreement with the idea that accumulation of ROS may drive the translocation of the SET complex, treatment of K562 cells with GzmA plus PFN caused a rapid nuclear relocation of the SET complex proteins starting at 5 min, the earliest time point analyzed (Figure 7B). In cells treated with GzmA alone or PFN alone, SET, pp32, and NM23-H1 remained cytosolic. The nuclear accumulation of SET, pp32, and NM23-H1 after GzmA treatment was associated with a decrease of the cytoplasmic level of these proteins. The GzmA cleavage product of SET was only detected in the nucleus of cells treated with both GzmA and PFN, suggesting that GzmA cleavage occurs mostly in the nucleus, where GzmA is known to concentrate (Fan et al., 2003b; Jans et al., 1998).

To prove that the ROS accumulation induced by GzmA treatment is responsible for SET complex nuclear translocation, we determined the subcellular localization of SET complex proteins in the absence or presence of Tiron (Figure 7C) or D1417 (data not shown). As in Figure 7B, in untreated K562 cells or cells treated with GzmA alone or PFN alone, SET, pp32, and NM23-H1 were concentrated in the cytoplasmic fraction, while, in cells exposed to GzmA plus PFN, the proteins appear in the nuclear fraction (Figure 7C). When K562 cells were treated with GzmA plus PFN in the presence of Tiron or D1417, however, nuclear translocation of SET, pp32, and NM23-H1 was blocked.

Immunostaining and confocal microscopy also demonstrated the translocation of NM23-H1 in HeLa cells after treatment with GzmA or H_2O_2 and its inhibition by the free radical scavenger Tiron. Untreated HeLa cells or cells treated with GzmA and/or PFN, or H_2O_2 in the presence or absence of Tiron, were stained with antibodies to NM23-H1 and histone H1. NM23-H1 was primarily perinuclear in untreated cells and in cells treated with GzmA, PFN, or Tiron alone (Figure 7D). In contrast, in cells treated with GzmA plus PFN or H_2O_2, much of NM23-H1 moved into the nucleus by 10 min and stained in a similar pattern as histone H1. Furthermore, Tiron pretreatment blocked NM23-H1 translocation induced by GzmA and PFN. SET staining under all these conditions mimicked NM23-H1 staining (data not shown). Taken together, these results demonstrate that the increase in intracellular ROS initiated by GzmA is responsible for the translocation of SET complex proteins, and that superoxide plays a key role in this process.

Discussion

Mitochondria play an important role in caspase-mediated apoptosis, in which disruption of MOM integrity releases a number of key intermembrane proteins, such as cytochrome c, that help activate apoptosis when released from the mitochondrion, despite the fact that they contribute to normal metabolic function and cell viability within the mitochondrion. Signs of mitochondrial metabolic dysfunction—increased ROS and loss of the membrane potential difference between the inner and outer membranes—are also hallmarks of apoptotic mitochondrial damage. However, increased ROS and loss of $\Delta\psi$, because they signal mitochondrial dysfunction, are characteristic of necrotic cell death as well. Although many of the critical molecules involved in mitochondrial pathways of apoptosis have been identified, how these different aspects of mitochondrial damage in caspase-dependent apoptosis fit together, as well as their relative importance and the molecular basis for their activity are still incompletely understood and controversial, despite extensive study (Green and Kroemer, 2004; Newmeyer and Ferguson-Miller, 2003). It has never been completely clear whether generation of ROS is central to apoptosis or merely a side effect of mitochondrial dysfunction.

In this study, we find that generation of ROS, particularly superoxide ion, is critical for the distinct caspase-independent cell death pathway triggered by the CTL and NK cell protease GzmA, which has all the morphological features of apoptosis (model shown in Figure 7E). The experiments in this study were performed by using recombinant human GzmA and GzmA-expressing cytotoxic T cells derived from both mice and humans assayed against a variety of mouse and human target cells. Our conclusions, therefore, are broadly applicable across targets and species. Pretreatment of mouse and human target cells with superoxide scavengers completely inhibits GzmA-mediated cell death. GzmA triggers mitochondrial damage with rapid increase in ROS and loss of $\Delta\psi$, but leaves the outer membrane intact so that cytochrome c and other apoptotic mediators do not escape. Moreover, this mitochondrial damage pathway is caspase independent, since it is not inhib-

(E) Critical role of mitochondrial damage in GzmA-mediated cell death. GzmA, delivered into the target cell by PFN, activates loss of mitochondrial transmembrane potential ($\Delta\psi$) and increased ROS, including superoxide ion (O_2^-). Superoxide triggers translocation of the ER-associated SET complex into the nucleus. The superoxide scavengers Tiron and D1417 can prevent this process. GzmA (through an unknown mechanism) also translocates to the nucleus. In the nucleus, GzmA cleaves SET, releasing the GzmA-activated DNase (NM23-H1) from inhibition, and also cleaves other SET complex proteins (Ape1 and HMG-2), the lamins, histone H1, and the tails from the core histones. Histone cleavage by GzmA opens up chromatin for efficient DNA damage by NM23-H1. (This model figure was adapted from a recent review of the GzmA pathway [Lieberman and Fan, 2003].)

ited by overexpression of bcl-2 or by pan-caspase inhibitors. In addition, we have begun to understand why ROS generation is critical for executing the GzmA apoptotic pathway. ROS triggers the nuclear translocation of the SET complex, an important target of GzmA. The SET complex contains the GzmA-activated DNase, NM23-H1, as well as its inhibitor, SET, which when cleaved by GzmA activates the DNase. Moreover, the rapid translocation of the SET complex in response to oxidative stress and its inhibition by superoxide scavengers lends support to our hypothesis that the SET complex is an oxidative stress response complex.

ROS generation was found to be critical not only for the GzmA pathway, but also for cell death induction via granule exocytosis by CTLs expressing GzmB in addition to GzmA. These findings were demonstrated by using a variety of CTLs from both humans and mice. Since GzmB activates caspase-dependent apoptosis (as well as caspase-independent cell death), this suggests that ROS generation may also be critical for some caspase-dependent apoptotic pathways in some cells. Previous studies have also suggested that blocking ROS generation can inhibit other forms of apoptosis, including that induced by death receptor ligation, cytokine withdrawal, and T lymphocyte activation-induced cell death (Chang et al., 1992; Hildeman et al., 1999; Hockenbery et al., 1993; Sandstrom et al., 1994). Taken together, these studies suggest that generation of ROS is often integral to apoptosis induction, not just an epiphenomenon. Our results suggest that the granule pathways of killer cell apoptosis require superoxide generation, while the death receptor pathways may not.

The molecular basis for caspase-independent mitochondrial damage by GzmA remains to be worked out. Mitochondrial damage requires the proteolytic activity of GzmA, since the catalytically inactive enzyme S-AGzmA does not induce mitochondrial damage (data not shown). It involves direct action of GzmA on a mitochondrial substrate since we could demonstrate increased ROS (Figure 1D) and loss of mitochondrial $\Delta\psi$ (not shown) by incubating isolated mitochondria only with GzmA. Several studies have suggested that two other Gzms (B and C) are also able to trigger increased ROS and loss of mitochondrial $\Delta\psi$ in a caspase-independent manner through an unknown mechanism. It is possible that these proteases all target the same mitochondrial protein.

Our results have therapeutic implications for clinical situations in which ebullient granule-mediated cytolytic activity by CTLs or NK cells has adverse consequences, such as in posttransplant graft versus host disease or autoimmunity. ROS scavengers or other antioxidants might be effective in these situations in inhibiting apoptosis induced by granule exocytosis. At some concentrations, these agents might selectively block the apoptotic effects of granule exocytosis, but leave other immune apoptotic pathways unaffected. For example, although granule exocytosis is the major pathway used by killer immune cells to eliminate viruses and cancer cells, engagement of cell death receptors, such as Fas, is thought to be important for terminating the immune response and controlling the survival of activated T cells. At the maximally tolerated concentration, superoxide scavengers tested in this study were able to inhibit granule exocytosis, but had no effect on Fas-mediated apoptosis of Jurkat T cells, despite previous reports of effectiveness of antioxidants at blocking Fas-mediated apoptosis (Malassagne et al., 2001). However, other work suggests that ROS generation may actually protect cells from Fas-mediated apoptosis (Aronis et al., 2003). We have found that ROS does not increase in Fas-treated Jurkat cells until after cells have externalized phosphatidyl serine and become permeabilized to PI (data not shown), suggesting that an increase in ROS is a late nonessential phenomenon in this pathway. However, the maximal concentration of antioxidants tolerated by Jurkat cells was not as high as was used to protect K562 or EL4 target cells from GzmA or CTL attack.

In this study, the superoxide scavengers were most effective not only at preventing ROS generation, but also at protecting cells from GzmA- and CTL-induced cell death. The PT pore inhibitors provided only partial protection. It is not clear whether this is because only some of the ROS generation requires opening of the PT pore or whether the inhibitors are not completely effective. NAC was significantly less effective than the superoxide scavengers at neutralizing ROS and was not able to protect cells from death. This may be because NAC acts more distally in the oxidative pathway, allowing some active superoxide to wreak its damage. Damage to the integrity of the plasma membrane is likely to be a key component of cell death, and the molecular basis for disruption of the plasma membrane is poorly understood. Our results perhaps suggest that superoxide damage to plasma membrane lipids may be an important component that can be blocked by superoxide scavengers, but not by antioxidants like NAC.

We previously postulated, based on the functions of its components, that the SET complex is involved in the oxidative stress repair response (Fan et al., 2003a, 2003b). Our finding here that the SET complex proteins translocate to the nucleus within a minute or two of peroxide treatment supports this hypothesis. We also previously found that the SET complex proteins, Ape1, SET, and NM23-H1, move into the nucleus of target cells within 5–20 min of initiating CTL granule release. We now find that the SET complex proteins move synchronously into the nucleus in response to different oxidative stresses. GzmA induces rapid ROS generation in targeted cells. Moreover, scavenging superoxide anions not only inhibits ROS build-up, but also blocks SET complex protein translocation. This suggests that the SET complex is triggered to translocate to the nucleus by ROS. The molecular basis for ROS induction of SET complex translocation requires further study. The synchronous translocation of SET, pp32, and NM23-H1 (as well as Ape1 [data not shown]) into the nucleus in response to peroxide and GzmA suggests that the SET complex translocates as a complex into the nucleus, although this remains unproven. We also have not studied whether the SET complex remains intact once in the nucleus. Since others have identified smaller, ~150 kDa, SET- and pp32-containing nuclear complexes involved in inhibiting histone acetylation and stabilizing AU-rich mRNAs (Brennan et al., 2000; Seo et al., 2001), it is possible that the SET complex partially disassembles in the nucleus. However, it is also pos-

sible that these multifunctional proteins participate in more than one complex. Isolation of nuclear SET complex(es) after peroxide treatment will provide a way to examine this question.

The rapidity of SET complex translocation within a minute or two in response to ROS generation may also help explain why the subcellular localization of SET complex proteins as visualized by immunofluorescence microscopy studies varies in the literature and depends on the fixation protocol (Beresford et al., 2001; Fan et al., 2002, 2003a, 2003b). During the time required for fixation, ROS may be generated, stimulating the SET complex to migrate to the nucleus. In all of our studies, we have been careful to require consistent results from subcellular fractionation and microscopy. In this study, we developed a specific staining protocol that avoids fixation to minimize possible artifacts.

Since the SET complex appears to translocate into the nucleus in response to oxidative stress, and since most forms of cell death involve ROS generation, we would expect to see SET complex translocation induced by other forms of apoptosis and necrosis. Preliminary experiments suggest that this is indeed the case. GzmA cleaves several of the SET complex proteins (Ape1, SET, and HMG-2) and destroys their normal functions, including base excision repair. At the same time, GzmA unleashes the endonuclease activity of NM23-H1, normally kept under control by SET, to damage DNA. If the role of the SET complex is to repair oxidative DNA damage and induce expression of repair response genes, then other apoptotic pathways might also find ways to disable the repair functions of the SET complex or transform its repair functions into mechanisms for promoting cell death.

Experimental Procedures

Cell Lines, Antibodies, and Reagents

Cells were grown in K10 medium (RPMI1640 supplemented with 10% fetal calf serum, 2 mM glutamine, 2 mM HEPES, 100 units/ml penicillin, 100 mg/ml streptomycin). Jurkat-bcl-2 and Jurkat-neo (kind gifts of John Reed [Torigoe et al., 1994]) were grown in the same medium with 0.4 mg/ml geneticin. CTL lines were generated from P14 (Pircher et al., 1989) and P14xGzmB$^{-/-}$ (Pham et al., 1996) mouse splenocytes activated with 1 μg/ml specific LCMV peptide gp33 (KAVYNFATC) for 1 hr, washed, and cultured in medium to which 25 IU/ml recombinant human IL-2 was added every other day beginning on day 2. Cell lines were used for experiments after 8–15 days of culture. Mice were backcrossed and maintained under specific pathogen-free conditions. Human LAK cells was generated from healthy donor peripheral blood mononuclear cells maintained in K10 plus 1000 IU/ml IL-2 for up to 10 days. A CMV-specific CTL line (98% CD3+, 80% CD8+) specific for an A2-restricted CMV epitope (NLVPMLATL, 50% of all cells tetramer+) was generated by stimulating normal donor PBMC twice with the cognate peptide (5 μg/ml; the second time by using autologous B-LCL stimulator cells) and culturing in medium containing 20 IU/ml IL-2 and 25 ng/ml IL-15. The following antibodies were used: cytochrome c (mouse mAb), apoptosis inducing factor (AIF), CD3ε-FITC, CD8-PE, CD107a-FITC, and annexin V-FITC (BD PharMingen, San Diego, CA); HtrA2, NM23-H1, and bcl-2 (Santa Cruz Biotechnology, Santa Cruz, CA); bid (rat mAb) (R&D Systems); histone H1 (mouse mAb) (Chemicon International); Fas (CH11, mouse mAb) (Immunotech); β-actin (mouse mAb) (Sigma-Aldrich, St Louis, MO), and cytochrome c oxidase IV (Molecular Probes, Eugene, OR). Anti-pp32 (RJ1) and rabbit antiserum to SET peptide 3–16 were produced as described (Beresford et al., 2001). Rabbit antiserum to endonuclease G was a gift of Dr. Xiaodong Wang (University of Texas Southwestern Medical Center). Bongkrekic acid (BA), Cyclosporine A (CsA), 4,5-dihydroxyl-1,3-benzene-disulfonic acid (Tiron), 3,5-dibromo-4-nitrosobenzenesulfonic acid (D1417), N-acetyl cysteine (NAC), staurosporine, and propidium iodide (PI) were from Sigma-Aldrich. HE and CellTrace Far Red DDAO-SE, Alexa488-conjugated donkey anti-mouse, and Alexa594-conjugated donkey anti-rabbit Igs were from Molecular Probes; caspase inhibitor peptides were from Calbiochem-Novabiochem, San Diego, CA; and the gag, gp33, and CMV peptides were synthesized and purified at the Tufts Peptide facility. GzmA and inactive S-AGzmA were expressed and purified as previously reported (Beresford et al., 1999). PFN and GzmB were purified from rat RNK-16 cells, and cells were loaded with sublytic concentrations of PFN as described (Shi et al., 1992; Shi et al., 2000).

Gzm and PFN Treatment

Cells were washed three times in HBSS and resuspended (2×10^4 cells in 60 μl final volume) in cell buffer (HBSS with 10 mM HEPES [pH 7.2], 0.4% BSA, 3 mM $CaCl_2$). A sublytic concentration of PFN (determined for each cell independently) and/or GzmA (1 μM or as indicated) or GzmB (1 μM or as indicated) was added, and the cells were cultured at 37°C for the indicated time. For some experiments, NP40 cell lysates obtained after 1 hr of incubation were analyzed by immunoblot for bid. For cell death assays, cells were stained 1 hr after PFN and/or Gzm treatment with annexin V and PI and were analyzed by flow cytometry as described (Friedman et al., 2000).

Intracellular ROS Production and Transmembrane Potential Loss

ROS production was monitored by adding 2 μM HE just before flow cytometry analysis to cells treated for 1 hr (or an indicated time) at 37°C. As a positive control, cells were exposed to 1%–5% H_2O_2. Changes in mitochondrial $\Delta\psi$ were monitored with the potentiometric dye JC-1 by using the Mitochondrial Membrane Potential Detection Kit (BioCarta US). As a positive control, cells were treated overnight with 0.1 μM staurosporine or cultured overnight following UV irradiation (100 μJ/cm^2 × 5 min). For inhibition experiments, cells were preincubated for 15–30 min with inhibitors at the concentrations indicated before adding PFN or Gzms. Flow cytometry analyses were performed by using a Becton Dickinson FACSCalibur flow cytometer and Cellquest Pro software.

Isolated Mitochondria Assays

Mitochondria and S100 supernatants were freshly prepared from mouse liver as described (Susin et al., 2000). Mitochondria (0.5 mg/ml protein) were incubated with or without S100 supernatant (1 mg/ml) plus Gzms at indicated concentrations in a total volume of 60 μl mitochondrial buffer (220 mM sucrose, 68 mM mannitol, 10 mM KCl, 5 mM KH_2PO_4, 2 mM $MgCl_2$, 0.5 mM EGTA, 5 mM succinate, 2 mM rotenone, 10 mM HEPES [pH 7.2]) for 30 min at 37°C. Mitochondria were stained with 150 μM HE for flow cytometry as described above. For detecting release of apoptogenic factors, after centrifugation at 760 × g for 5 min, the mitochondrial pellet and supernatant fractions were analyzed by immunoblot.

ROS Production by Confocal Microscopy

EL4 target cells (2×10^6) were pulsed with 0.5 μg/ml specific LCMV peptide gp33 (KAVYNFATC) or an irrelevant HIV gag peptide (SLYNTVATL) for 1 hr at 37°C, and then washed in Ca^{2+}-free HBSS. The target cells were stained with 10 μM CellTrace Far Red DDAO-SE for 15 min at 37°C, then washed in Ca^{2+}-free HBSS. Simultaneously, syngeneic P14xGzmB$^{-/-}$ CD8$^+$ effector cells (5×10^6) were stained with 10 μg/ml FITC-CD3ϵ for 30 min at room temperature and washed. The effector cells were mixed with the EL4 targets in a 5:1 ratio in Ca^{2+}-free HBSS, and the conjugates were allowed to settle onto poly-lysine-coated slides for 30 min at 37°C. The slides were washed twice and incubated for 1 min with warm HBSS with 2 μM HE containing either 10 mM Ca^{2+} or 10 mM EGTA. After a rapid wash in HBSS, the slides were mounted and fluorescence was observed immediately by using a Bio-Rad Radiance 2000 laser-scanning confocal microscope.

Degranulation Assay

CTL degranulation was assayed as previously reported (Betts et al., 2003), with minor modifications. EL4 cells, pulsed with irrelevant HIV gag peptide or the specific LCMV peptide gp33 as described above, were mixed in a 5:1 target:effector ratio with P14xGzmB$^{-/-}$ CD8^{+} effector cells in the presence of 1 μg/ml CD107a-FITC, 1 μg/ml anti-CD28, and (1 μg/ml) anti-CD49d for 6 hr at 37°C. The cells were washed, fixed with 3.7% paraformaldehyde, and further stained with CD8-PE. Flow cytometry analysis for cell surface CD107a expression was performed on gated lymphocytes.

SET Complex Translocation

K562 cells were washed three times in HBSS, and 2–4 × 10^5 cells were incubated with either 1% H_2O_2 or sublytic PFN and/or GzmA (1 μM) for the indicated time at 37°C in the absence or presence of 80 mM Tiron. Washed cells were lysed with 0.5% NP40 lysis buffer containing protease inhibitors. After centrifugation at 3000 rpm for 5 min, the supernatant (cytoplasmic fraction) was separated from the pellet (nuclear fraction). The nuclear pellet was further washed and resuspended in NP40 lysis buffer containing 1% Triton X-100 and briefly sonicated. The fractions were resolved by immunoblot.

NM23-H1 Translocation by Confocal Microscopy

HeLa cells (0.4 × 10^5) grown overnight on cover slides were washed with HBSS and then left untreated or treated for 5–10 min at 37°C with H_2O_2, PFN, and/or GzmA in the presence or absence of Tiron as above. After an additional wash, unfixed cells were incubated for 30 min at room temperature in 1× permeabilization/wash (P/W) buffer (DB Bioscience) containing 10% donkey normal serum and then incubated with antibodies in the same buffer for 1 hr at room temperature. After three washes in P/W buffer, the cells were incubated with 1–2 mg/ml Alexa594-conjugated donkey anti-rabbit Ig and Alexa488-conjugated donkey anti-mouse Ig for 1 hr at room temperature. After further washes, cover slides were mounted, and the cells were observed for fluorescence by confocal microscopy as described above.

Cytotoxicity Assays

For mouse experiments, EL4 target cells (2 × 10^6) were incubated with 0.5 μg/ml LCMV gp33 peptide for 1 hr in the presence of 100 μCi/ml $Na_2{}^{51}CrO_4$ at 37°C. After washing, 2 × 10^3 target cells were preincubated or not for 15–30 min at 37°C in triplicate microtiter wells with the indicated inhibitor. Cells were then mixed with indicated P14 or P14GzmB$^{-/-}$ effector cells at a 50:1 effector:target ratio in 100 μl K10 medium and incubated at 37°C for 6 hr. For human studies, assay was performed as described above, but with K562 cells coated with 5 μg/ml conA as targets of human LAK cells or with autologous B-LCL pulsed with 5 μg/ml CMV peptide as targets of a CMV-specific CTL line. After centrifugation at 760 × g for 5 min, 45 μl supernatant was counted on a TopCount (Packard Instrument Company). Specific release is defined as ([cpm – spontaneous release]/[total release – spontaneous release]) × 100. In all cases, background cytolysis of unpulsed, control targets was <5%. Fas-mediated apoptosis was triggered by incubating Jurkat cells with 1 μg/ml CH11 antibody for 6 hr.

Supplemental Data

Supplemental Experimental Procedures are available with this article online at http://www.immunity.com/cgi/content/full/22/3/355/DC1/.

Acknowledgments

We thank Dipanjan Chowdhury for a critical review of the manuscript, Francisco Navarro for human CTL lines, Lianfa Shi and Deli He for preparing PFN, Patricia McCaffrey for editorial assistance, and members of the laboratory for helpful suggestions. This work was supported by National Institutes of Health grant AI45587 (J.L.).

Received: October 7, 2004
Revised: January 19, 2005
Accepted: February 2, 2005
Published: March 22, 2005

References

Alimonti, J.B., Shi, L., Baijal, P.K., and Greenberg, A.H. (2001). Granzyme B induces BID-mediated cytochrome c release and mitochondrial permeability transition. J. Biol. Chem. *276*, 6974–6982.

Aronis, A., Melendez, J.A., Golan, O., Shilo, S., Dicter, N., and Tirosh, O. (2003). Potentiation of Fas-mediated apoptosis by attenuated production of mitochondria-derived reactive oxygen species. Cell Death Differ. *10*, 335–344.

Barry, M., Heibein, J.A., Pinkoski, M.J., Lee, S.F., Moyer, R.W., Green, D.R., and Bleackley, R.C. (2000). Granzyme B short-circuits the need for caspase 8 activity during granule-mediated cytotoxic T-lymphocyte killing by directly cleaving Bid. Mol. Cell. Biol. *20*, 3781–3794.

Beresford, P.J., Kam, C.M., Powers, J.C., and Lieberman, J. (1997). Recombinant human granzyme A binds to two putative HLA-associated proteins and cleaves one of them. Proc. Natl. Acad. Sci. USA *94*, 9285–9290.

Beresford, P.J., Xia, Z., Greenberg, A.H., and Lieberman, J. (1999). Granzyme A loading induces rapid cytolysis and a novel form of DNA damage independently of caspase activation. Immunity *10*, 585–594.

Beresford, P.J., Zhang, D., Oh, D.Y., Fan, Z., Greer, E.L., Russo, M.L., Jaju, M., and Lieberman, J. (2001). Granzyme A activates an endoplasmic reticulum-associated caspase-independent nuclease to induce single-stranded DNA nicks. J. Biol. Chem. *276*, 43285–43293.

Betts, M.R., Brenchley, J.M., Price, D.A., De Rosa, S.C., Douek, D.C., Roederer, M., and Koup, R.A. (2003). Sensitive and viable identification of antigen-specific CD8+ T cells by a flow cytometric assay for degranulation. J. Immunol. Methods *281*, 65–78.

Brennan, C.M., Gallouzi, I.E., and Steitz, J.A. (2000). Protein ligands to HuR modulate its interaction with target mRNAs in vivo. J. Cell Biol. *151*, 1–14.

Chang, D.J., Ringold, G.M., and Heller, R.A. (1992). Cell killing and induction of manganous superoxide dismutase by tumor necrosis factor-alpha is mediated by lipoxygenase metabolites of arachidonic acid. Biochem. Biophys. Res. Commun. *188*, 538–546.

Demple, B., Herman, T., and Chen, D.S. (1991). Cloning and expression of APE, the cDNA encoding the major human apurinic endonuclease: definition of a family of DNA repair enzymes. Proc. Natl. Acad. Sci. USA *88*, 11450–11454.

Du, C., Fang, M., Li, Y., Li, L., and Wang, X. (2000). Smac, a mitochondrial protein that promotes cytochrome c-dependent caspase activation by eliminating IAP inhibition. Cell *102*, 33–42.

Fan, Z., Beresford, P.J., Zhang, D., and Lieberman, J. (2002). HMG2 interacts with the nucleosome assembly protein SET and is a target of the cytotoxic T-lymphocyte protease granzyme A. Mol. Cell. Biol. *22*, 2810–2820.

Fan, Z., Beresford, P.J., Oh, D.Y., Zhang, D., and Lieberman, J. (2003a). Tumor suppressor NM23–H1 is a Granzyme A-activated DNase during CTL-mediated apoptosis, and the nucleosome assembly protein SET is its inhibitor. Cell *112*, 659–672.

Fan, Z., Beresford, P.J., Zhang, D., Xu, Z., Novina, C.D., Yoshida, A., Pommier, Y., and Lieberman, J. (2003b). Cleaving the oxidative repair protein Ape1 enhances cell death mediated by granzyme A. Nat. Immunol. *4*, 145–153.

Friedman, R.S., Frankel, F.R., Xu, Z., and Lieberman, J. (2000). Induction of human immunodeficiency virus (HIV)-specific CD8 T-cell responses by Listeria monocytogenes and a hyperattenuated Listeria strain engineered to express HIV antigens. J. Virol. *74*, 9987–9993.

Green, D.R., and Kroemer, G. (2004). The pathophysiology of mitochondrial cell death. Science *305*, 626–629.

Gross, A., Yin, X.M., Wang, K., Wei, M.C., Jockel, J., Milliman, C.,

Erdjument-Bromage, H., Tempst, P., and Korsmeyer, S.J. (1999). Caspase cleaved BID targets mitochondria and is required for cytochrome c release, while BCL-XL prevents this release but not tumor necrosis factor-R1/Fas death. J. Biol. Chem. *274*, 1156–1163.

Hegde, R., Srinivasula, S.M., Zhang, Z., Wassell, R., Mukattash, R., Cilenti, L., DuBois, G., Lazebnik, Y., Zervos, A.S., Fernandes-Alnemri, T., and Alnemri, E.S. (2002). Identification of Omi/HtrA2 as a mitochondrial apoptotic serine protease that disrupts inhibitor of apoptosis protein-caspase interaction. J. Biol. Chem. *277*, 432–438.

Heibein, J.A., Barry, M., Motyka, B., and Bleackley, R.C. (1999). Granzyme B-induced loss of mitochondrial inner membrane potential (Delta Psi m) and cytochrome c release are caspase independent. J. Immunol. *163*, 4683–4693.

Heibein, J.A., Goping, I.S., Barry, M., Pinkoski, M.J., Shore, G.C., Green, D.R., and Bleackley, R.C. (2000). Granzyme B-mediated cytochrome c release is regulated by the bcl-2 family members bid and Bax. J. Exp. Med. *192*, 1391–1402.

Heusel, J.W., Wesselschmidt, R.L., Shresta, S., Russell, J.H., and Ley, T.J. (1994). Cytotoxic lymphocytes require granzyme B for the rapid induction of DNA fragmentation and apoptosis in allogeneic target cells. Cell *76*, 977–987.

Hildeman, D.A., Mitchell, T., Teague, T.K., Henson, P., Day, B.J., Kappler, J., and Marrack, P.C. (1999). Reactive oxygen species regulate activation-induced T cell apoptosis. Immunity *10*, 735–744.

Hockenbery, D.M., Oltvai, Z.N., Yin, X.M., Milliman, C.L., and Korsmeyer, S.J. (1993). Bcl-2 functions in an antioxidant pathway to prevent apoptosis. Cell *75*, 241–251.

Jans, D.A., Briggs, L.J., Jans, P., Froelich, C.J., Parasivam, G., Kumar, S., Sutton, V.R., and Trapani, J.A. (1998). Nuclear targeting of the serine protease granzyme A (fragmentin-1). J. Cell Sci. *111*, 2645–2654.

Johnson, H., Scorrano, L., Korsmeyer, S.J., and Ley, T.J. (2003). Cell death induced by granzyme C. Blood *101*, 3093–3101.

Kluck, R.M., Bossy-Wetzel, E., Green, D.R., and Newmeyer, D.D. (1997). The release of cytochrome c from mitochondria: a primary site for Bcl-2 regulation of apoptosis. Science *275*, 1132–1136.

Krippner, A., Matsuno-Yagi, A., Gottlieb, R.A., and Babior, B.M. (1996). Loss of function of cytochrome c in Jurkat cells undergoing Fas-mediated apoptosis. J. Biol. Chem. *271*, 21629–21636.

Kroemer, G., Dallaporta, B., and Resche-Rigon, M. (1998). The mitochondrial death/life regulator in apoptosis and necrosis. Annu. Rev. Physiol. *60*, 619–642.

Li, H., Zhu, H., Xu, C., and Yuan, J. (1998). Cleavage of BID by caspase 8 mediates the mitochondrial damage in the Fas pathway of apoptosis. Cell *94*, 491–501.

Lieberman, J., and Fan, Z. (2003). Nuclear war: the granzyme A-bomb. Curr. Opin. Immunol. *15*, 553–559.

Luo, X., Budihardjo, I., Zou, H., Slaughter, C., and Wang, X. (1998). Bid, a Bcl2 interacting protein, mediates cytochrome c release from mitochondria in response to activation of cell surface death receptors. Cell *94*, 481–490.

Ma, D., Xing, Z., Liu, B., Pedigo, N.G., Zimmer, S.G., Bai, Z., Postel, E.H., and Kaetzel, D.M. (2002). NM23-H1 and NM23-H2 repress transcriptional activities of nuclease-hypersensitive elements in the platelet-derived growth factor-A promoter. J. Biol. Chem. *277*, 1560–1567.

MacDonald, G., Shi, L., Vande Velde, C., Lieberman, J., and Greenberg, A.H. (1999). Mitochondria-dependent and -independent regulation of granzyme B-induced apoptosis. J. Exp. Med. *189*, 131–144.

Malassagne, B., Ferret, P.J., Hammoud, R., Tulliez, M., Bedda, S., Trebeden, H., Jaffray, P., Calmus, Y., Weill, B., and Batteux, F. (2001). The superoxide dismutase mimetic MnTBAP prevents Fas-induced acute liver failure in the mouse. Gastroenterology *121*, 1451–1459.

Marchetti, P., Castedo, M., Susin, S.A., Zamzami, N., Hirsch, T., Macho, A., Haeffner, A., Hirsch, F., Geuskens, M., and Kroemer, G. (1996). Mitochondrial permeability transition is a central coordinating event of apoptosis. J. Exp. Med. *184*, 1155–1160.

Martins, L.M., Iaccarino, I., Tenev, T., Gschmeissner, S., Totty, N.F., Lemoine, N.R., Savopoulos, J., Gray, C.W., Creasy, C.L., Dingwall, C., and Downward, J. (2002). The serine protease Omi/HtrA2 regulates apoptosis by binding XIAP through a reaper-like motif. J. Biol. Chem. *277*, 439–444.

Newmeyer, D.D., and Ferguson-Miller, S. (2003). Mitochondria: releasing power for life and unleashing the machineries of death. Cell *112*, 481–490.

Parrish, J., Li, L., Klotz, K., Ledwich, D., Wang, X., and Xue, D. (2001). Mitochondrial endonuclease G is important for apoptosis in *C. elegans*. Nature *412*, 90–94.

Pham, C.T., MacIvor, D.M., Hug, B.A., Heusel, J.W., and Ley, T.J. (1996). Long-range disruption of gene expression by a selectable marker cassette. Proc. Natl. Acad. Sci. USA *93*, 13090–13095.

Pircher, H., Burki, K., Lang, R., Hengartner, H., and Zinkernagel, R.M. (1989). Tolerance induction in double specific T-cell receptor transgenic mice varies with antigen. Nature *342*, 559–561.

Sandstrom, P.A., Mannie, M.D., and Buttke, T.M. (1994). Inhibition of activation-induced death in T cell hybridomas by thiol antioxidants: oxidative stress as a mediator of apoptosis. J. Leukoc. Biol. *55*, 221–226.

Seo, S., McNamara, P., Heo, S., Turner, A., Lane, W.S., and Chakravarti, D. (2001). Regulation of histone acetylation and transcription by INHAT, a human cellular complex containing the Set oncoprotein. Cell *104*, 119–130.

Shi, L., Kraut, R.P., Aebersold, R., and Greenberg, A.H. (1992). A natural killer cell granule protein that induces DNA fragmentation and apoptosis. J. Exp. Med. *175*, 553–566.

Shi, L., Yang, X., Froelich, C.J., and Greenberg, A.H. (2000). Purification and use of granzyme B. Methods Enzymol. *322*, 125–143.

Shikama, N., Chan, H.M., Krstic-Demonacos, M., Smith, L., Lee, C.W., Cairns, W., and La Thangue, N.B. (2000). Functional interaction between nucleosome assembly proteins and p300/CREB-binding protein family coactivators. Mol. Cell. Biol. *20*, 8933–8943.

Susin, S.A., Lorenzo, H.K., Zamzami, N., Marzo, I., Snow, B.E., Brothers, G.M., Mangion, J., Jacotot, E., Costantini, P., Loeffler, M., et al. (1999). Molecular characterization of mitochondrial apoptosis-inducing factor. Nature *397*, 441–446.

Susin, S.A., Larochette, N., Geuskens, M., and Kroemer, G. (2000). Purification of mitochondria for apoptosis assays. Methods Enzymol. *322*, 205–208.

Sutton, V.R., Davis, J.E., Cancilla, M., Johnstone, R.W., Ruefli, A.A., Sedelies, K., Browne, K.A., and Trapani, J.A. (2000). Initiation of apoptosis by granzyme B requires direct cleavage of bid, but not direct granzyme B-mediated caspase activation. J. Exp. Med. *192*, 1403–1414.

Thomas, D.A., Scorrano, L., Putcha, G.V., Korsmeyer, S.J., and Ley, T.J. (2001). Granzyme B can cause mitochondrial depolarization and cell death in the absence of BID, BAX, and BAK. Proc. Natl. Acad. Sci. USA *98*, 14985–14990.

Torigoe, T., Millan, J.A., Takayama, S., Taichman, R., Miyashita, T., and Reed, J.C. (1994). Bcl-2 inhibits T-cell-mediated cytolysis of a leukemia cell line. Cancer Res. *54*, 4851–4854.

van Loo, G., Schotte, P., van Gurp, M., Demol, H., Hoorelbeke, B., Gevaert, K., Rodriguez, I., Ruiz-Carrillo, A., Vandekerckhove, J., Declercq, W., et al. (2001). Endonuclease G: a mitochondrial protein released in apoptosis and involved in caspase-independent DNA degradation. Cell Death Differ. *8*, 1136–1142.

van Loo, G., van Gurp, M., Depuydt, B., Srinivasula, S.M., Rodriguez, I., Alnemri, E.S., Gevaert, K., Vandekerckhove, J., Declercq, W., and Vandenabeele, P. (2002). The serine protease Omi/HtrA2 is released from mitochondria during apoptosis. Omi interacts with caspase-inhibitor XIAP and induces enhanced caspase activity. Cell Death Differ. *9*, 20–26.

Verhagen, A.M., Ekert, P.G., Pakusch, M., Silke, J., Connolly, L.M., Reid, G.E., Moritz, R.L., Simpson, R.J., and Vaux, D.L. (2000). Identi-

fication of DIABLO, a mammalian protein that promotes apoptosis by binding to and antagonizing IAP proteins. Cell *102*, 43–53.

Verhagen, A.M., Silke, J., Ekert, P.G., Pakusch, M., Kaufmann, H., Connolly, L.M., Day, C.L., Tikoo, A., Burke, R., Wrobel, C., et al. (2002). HtrA2 promotes cell death through its serine protease activity and its ability to antagonize inhibitor of apoptosis proteins. J. Biol. Chem. *277*, 445–454.

Yang, J., Liu, X., Bhalla, K., Kim, C.N., Ibrado, A.M., Cai, J., Peng, T.I., Jones, D.P., and Wang, X. (1997). Prevention of apoptosis by Bcl-2: release of cytochrome c from mitochondria blocked. Science *275*, 1129–1132.

Zamzami, N., Marchetti, P., Castedo, M., Hirsch, T., Susin, S.A., Masse, B., and Kroemer, G. (1996). Inhibitors of permeability transition interfere with the disruption of the mitochondrial transmembrane potential during apoptosis. FEBS Lett. *384*, 53–57.

Zhang, D., Beresford, P.J., Greenberg, A.H., and Lieberman, J. (2001a). Granzymes A and B directly cleave lamins and disrupt the nuclear lamina during granule-mediated cytolysis. Proc. Natl. Acad. Sci. USA *98*, 5746–5751.

Zhang, D., Pasternack, M.S., Beresford, P.J., Wagner, L., Greenberg, A.H., and Lieberman, J. (2001b). Induction of rapid histone degradation by the cytotoxic T lymphocyte protease granzyme A. J. Biol. Chem. *276*, 3683–3690.

Note Added in Proof

In agreement with our results, caspase-independent mitochondrial damage was recently described for CTL generated from GzmB$^{-/-}$ mice (Pardo et al., 2004). These authors also found that NAC could inhibit ROS, but not block GzmA-induced cell death.

Pardo, J., Bosque, A., Brehm, R., Wallich, R., Naval, J., Mullbacher, A., Anel, A., and Simon, M.M. (2004). Apoptotic pathways are selectively activated granzyme A and/or granzyme B in CTL-mediated target cell lysis. J. Cell Biol. *167*, 457–468.